-Supporting Information-

Tuneable Metamaterial-like Platforms for Surface Enhanced Raman Scattering *via* Three-Dimensional Block Copolymer Based Nanoarchitectures

Carl Banbury[1], Jonathan James Stanley Rickard[1,2], Sumeet Mahajan[3] and Pola Goldberg Oppenheimer[1,*]

[1] *School of Chemical Engineering, College of Engineering and Physical Sciences, University of Birmingham, Birmingham, B15 2TT, UK*
[2] *Department of Physics, Cavendish Laboratory, University of Cambridge, JJ Thomson Avenue, Cambridge, CB3 0HE, UK*
[3] *Department of Chemistry and the Institute for Life sciences, University of Southampton, University Road, Southampton, SO17 1BJ, UK*

[*] E-mail: GoldberP@bham.ac.uk

S1: Depth/Thickness Characterisation of the Electrdeposited Gold

Using the electrodeposition, thicknesses ranging from fractions of a template layer to several template layers can be obtained by adjusting the deposition time. At our experimental conditions, with the nucleation step consisting of 3 CV scans at a scan rate of 50mVs^{-1} and a deposition step at a fixed potential of -0.8V (*vs.* SCE, where maximum deposition efficiency occurs) for 100s (reaction kinetics-controlled region followed by a mass transport-controlled region, featuring a cathodic peak characteristic of diffusion-controlled electroplating processes) is known to yield a final thickness of 200±30nm. [Estrine, E.C. *et* al. *J. Electrochem. Chem.* **2014**, 161, D687; Universal Metal Finishing Guidebook. *Elsevier*, **2013**]

Based on the Faraday-Couloumb's Law, [Randles, J.E.B. *Trans. Faraday Soc.* **1948**, 327] the coating thickness can be stabilized for each metal by time and, under constant circumstances with constant current density (I), thickness rate of the coating (dX) develops related to time which is described through Equation [1]:

$$\frac{dx}{dt} = \frac{M_w I \varphi}{\rho A z F} \qquad [1]$$

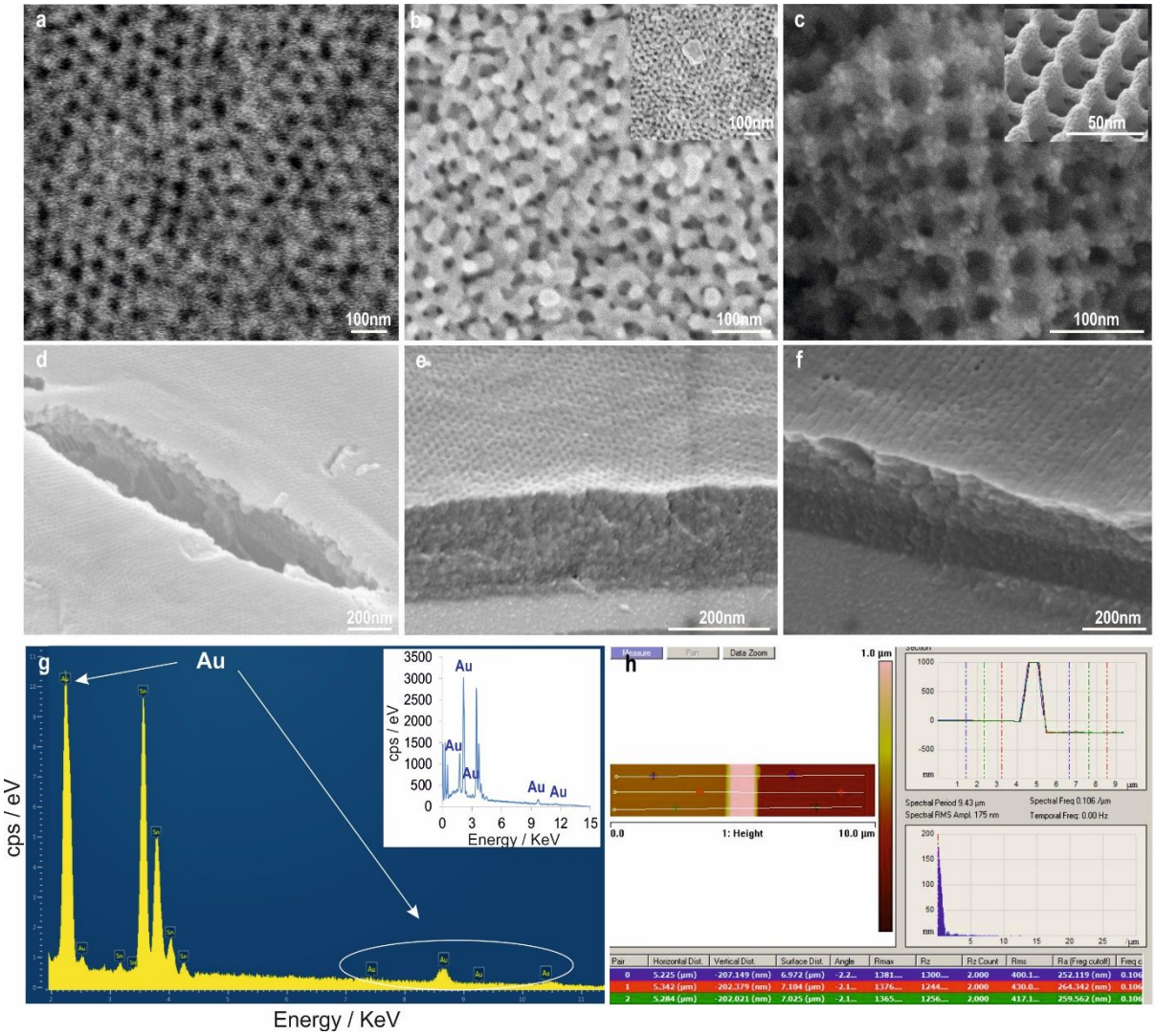

Supplementary Figure S1. (a). Low-angle back-scattered top-view SEM images of non-plated (a) *versus* the Au replicated (b-c) gyroid morphologies and the cross-sectional LAB-SEM profile images of gyroid and cylinder morphologies (d-f), electrochemically filled to depths of 200-230nm, with occasional overgrowth (above the thickness of the nano-morphology) appearing as florets of gold in several areas (b, inset) and the remaining polymer matrix was removed by exposing the material to 254nm UV etching. (g). EDX profile analysis reveals dominant Au peaks (highlighted with arrows) and given it interaction volume (at 5keV electron beam penetration depth is ~500nm), it also relevels occasional peaks of indium from the undelaying

ITO glass. (h). AFM height (left hand-side) and the corresponding cross-sectional depth profiles (right-hand side) of as-plated Au nanolayer (no BCP structure) highlighting 3 random locations on the substrate with an average heights of 203nm at set plating conditions. The AFM height images were acquired by plating the Au layer (left hand-side of the AFM height image) and subsequently, scalpel removal of the deposited gold, revealing bare substrate (right hand-side of the AFM height image) and creating the 'step-profile' enabling the characterisation of the depth profiles.

where, M_w is the molar weight of materials, (φ) current efficiency, ρ density of the sheeted layer, A deposited space, z the number of transferred electrons, and F is Faraday constant. Therefore, thickness (x) = $[It M_w \varphi]/[96485 \rho A z]$. Hence, at the current efficiency of 100% with the current density of 2mA/cm^2 at 0.8V *vs.* SCE at our experimental conditions, the plating rate is 120nm/min. Therefore, the calculated gold plated thickness is 200nm (for 100s). [Estrine, E.C. *et* al. *Journal of Electrochemical Chemistry* **2014**, 161, D687] and the deposited thickness can be altered from several single layers up to hundreds micrometres.

S2: Enhancement Factor Reproducibility

The reproducibility of the enhancement factor was obtained from 10 random areas for each of the four morphologies with the corresponding confidence intervals.

a

	Area on Substrate	Average Intensity / Counts mW^{-1}	Enhancement Factor	Relative Enhancement
FSG				
	1	35136.0	6.59E+07	1.03084
	2	43664.9	8.19E+07	1.28106
	3	39405.0	7.39E+07	1.15608
	4	42139.3	7.90E+07	1.23630
	5	53449.3	1.00E+08	1.54261
	6	52579.8	9.86E+07	1.54261
	7	47614.1	8.93E+07	1.39693
	8	46284.5	8.68E+07	1.35792
	9	43803.5	8.21E+07	1.28513
	10	34084.9	6.39E+07	1.00000
	Average		**8.22E+07**	
	STDEV		**1.22E+07**	

b

MCYL				
	1	30999.3	5.81E+07	1.00711
	2	32972.2	6.18E+07	1.10859
	3	34123.0	6.40E+07	1.10859
	4	36445.7	6.83E+07	1.18405
	5	30780.6	5.77E+07	1.00000
	6	37537.5	7.04E+07	1.21952
	7	43235.8	8.11E+07	1.40464
	8	43746.9	8.20E+07	1.42125
	9	31598.5	5.92E+07	1.02657
	10	32665.3	6.12E+07	1.06123
	Average		**6.64E+07**	
	STDEV		**8.99E+06**	

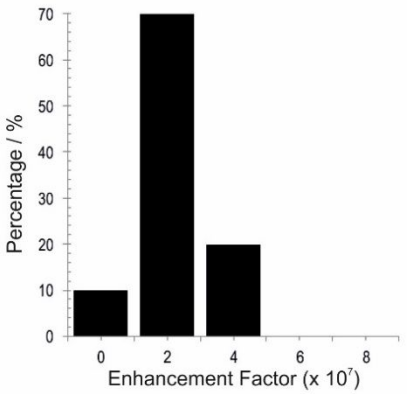

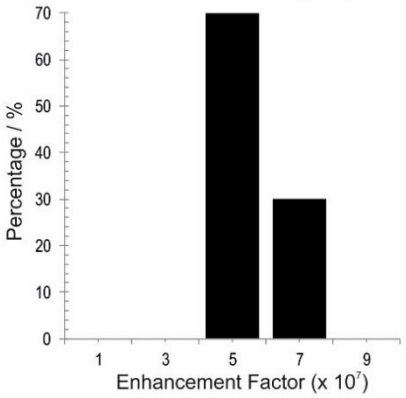

c

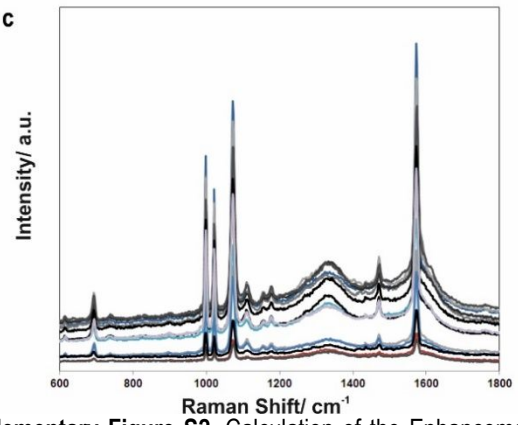

d

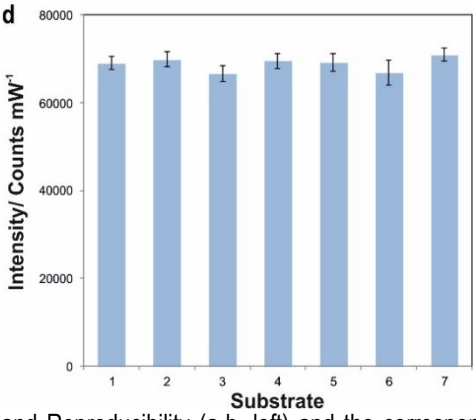

Supplementary Figure S2. Calculation of the Enhancement Factor and Reproducibility (a-b, left) and the corresponding narrowly distributed EF values (all around x10^7) for the FSG (a, right) and MCYL (b, right) morphologies. (c). Three different

substrates at 4-7 locations, under identical experimental conditions using BT monolayer as a standard probe analyte, yielded reproducible relative SERS intensities with variations of less than 9% in relative STDEV and less than 5.5% in terms of the relative peak intensities. (d). SERS signal of the peaks at 1070cm^{-1} of BT from 7 randomly selected positions on the substrates.

The limits of agreement and a range within which we expect 95% of future differences in measurements between each two substrates to lie, are calculated by first, establishing the mean and the STDEV for 10 areas across each substrate and subsequently, for the normally distributed data, the confidence interval limits for the EF values were calculated according to the: mean difference -1.96×STDEV (differences) and mean difference + 1.96×STDEV (differences). The EF values are narrowly distributed around the average of $8.2\times10^7 \pm 1.2\times10^7$, $4.5\times10^7 \pm 2.3\times10^7$, $6.6\times10^7 \pm 8.9\times10^6$ and $3.5\times10^6 \pm 1.3\times10^6$ for FSG (**Fig. S2, a; left hand-side**), CYL, MCYL (**Fig.S2, b; left hand-side**) and DG, accordingly.

The enhancement factors of the FSG-SERS substrates (**Fig.S2, a; right hand-side**) and MCYL-SERS substrates (**Fig.S2, b; right hand-side**) (n=10) show a narrow distribution with an average enhancement on the scale of (6-9) x10^7 (excluding one single area). Importantly, all EFs are on the same order of magnitude of x10^7 (for FSG, MCYL and CYL) and x10^6 (for DG) with the small variation in the pre-factor values. This confirms high-signal reproducibility over large areas in particular, as SERS EFs are typically considered very similar even when they show a nearly 1 order of magnitude difference [*e.g.,* Ansar, S.M. *et* al. *Phys. Chem. Lett.* **2012**, 3, 560]. SERS spectra of benzenethiol (**Fig.S2, c**) and intensities of the peaks at 1070cm^{-1} (**Fig.S2, d**) on 7 MCYL substrates across several random locations on each, with a 785nm laser and a 10s integration time, demonstrate reliable signal and substrate reproducibility. Repeatable SERS response was obtained from the surfaces with relative standard deviation values of less than 8.7% in the framework of one sample (error bars) and between the different samples (height of the bars).

S3: SERS Performance of the BCP-based Nanomorphologies Using R6G as Raman Probe

SERS performance of the four fabricated nanostructures was also evaluated with of 10μM R6G (P_{laser} = 3mW, t =10s) on each gold nanosurface (**Fig. S3, a**) at excitation wavelengths of 633 (grey) and 785nm (black).

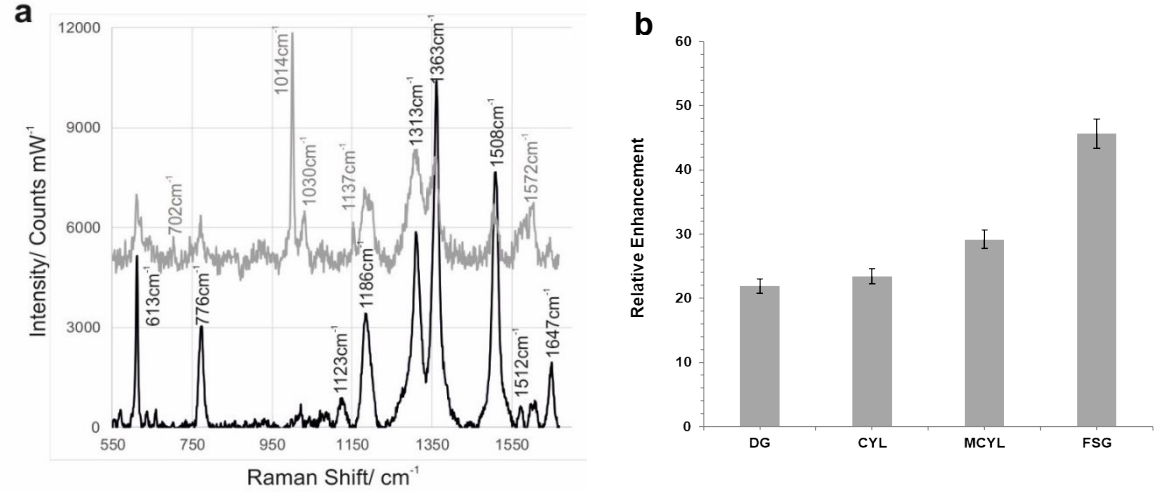

Supplementary Figure S3. (a). Representative SERS spectra of R6G recorded from substrates excited with a 633nm (grey) and 785 lasers (black) with typical Raman bands at 1363 and 1508cm^{-1} of the aromatic C-C stretching. (b). Relative SERS enhancement of the 1363cm^{-1} peak with the highest signal enhancement obtained for the FSG with 785nm followed by MCYL.

The marked peaks correspond to the Raman lines for R6G. SERS spectra exhibit difference in intensity and in certain enhanced Raman peaks at each excitation wavelength. While strong representative Raman bands at 613, 776, 1313, 1363 and 1508cm^{-1}, corresponding to the C-C-C in-plane ring bending, C-H out-of-plane bending and the aromatic C-C stretching, accordingly, are observed under excitation of both 633 and 785nm, at the shorter laser wavelength of 633nm additional Raman bands, of 1014, 1030, 1137 and 1572cm^{-1} are also enhanced, while the 1123 cm^{-1} (C-H in-plane bending) and 1647cm^{-1} (aromatic C-C stretching) peaks are further enhanced at 785nm excitation laser only. The absolute enhancement factor (EF) for all four nano-morphologies was found to be on the order of 10^7 with the FSG, followed by the MCYL, outperforming all the other nanostructures at 785nm, similarly to the case of BT (**Fig. S3, b**).